International Journal of Energy Production and Management
https://www.acadlore.com/journals/IJEPM

Solar-Powered Electrification and Hydrogen Integration for Decarbonising the Glass Industry

Lorenzo Miserocchi*, Alessandro Franco

Dipartimento di Ingegneria dell'Energia, dei Sistemi, del Territorio e delle Costruzioni (DESTEC), Università di Pisa, 56122 Pisa, Italy

* Correspondence: Lorenzo Miserocchi (lorenzo.miserocchi@ing.unipi.it)

Received: 09-05-2025 **Revised:** 11-15-2025 **Accepted:** 12-18-2025

Citation: L. Miserocchi and A. Franco, "Solar-powered electrification and hydrogen integration for decarbonising the glass industry," *Int. J. Energy Prod. Manag.*, vol. 10, no. 4, pp. 645–655, 2025. https://doi.org/10.56578/ijepm100406.

© 2025 by the author(s). Licensee Acadlore Publishing Services Limited, Hong Kong. This article can be downloaded for free, and reused and quoted with a citation of the original published version, under the CC BY 4.0 license.

Abstract: Deeper penetration of renewable energy is essential for decarbonising the glass industry, but balancing its intermittent nature with the sector's continuous high process heat demand remains challenging. Hybrid glass furnaces offer a promising solution by combining direct electrification with fuel switching to green hydrogen. This paper quantifies the viability of increased boosting levels in hybrid furnaces, identifying threshold conditions for profitability and sustainability at an electricity-to-natural-gas price ratio of 1.5 and an electricity emissions factor of 0.3 tCO_2/MWh. Subsequently, it investigates the economic and environmental impact of varying solar energy availability on decarbonising the energy supply of a representative 300 t/d oxyfuel container glass furnace equipped with solar plants and electrolysers of varying sizes. In the direct integration configuration, average melting cost savings and emission reductions reach 28.1%, and 18.8% for a 1:1 ratio between nominal furnace energy demand and solar generation. In a hydrogen integration configuration, average melting cost savings and emission reductions rise to 42.5% and 48.0%, with peak cost savings of 46.5%. Full energy self-sufficiency is achieved for solar overgeneration of around 36–40%, corresponding to a solar plant and electrolyser capacity of 150 MW and 45 MW. These general guidelines are meant to provide support for the design of low-carbon glass furnaces while minimising burdens on the broader energy system.

Keywords: Solar energy; Decarbonisation; Glass industry; Hard-to-abate industry; Electrification; Hydrogen

1 Introduction

The glass industry is a relevant energy-intensive and hard-to-abate sector, with total energy consumption estimated at approximately 350 PJ in the EU [1], 200 PJ in the US [2], and 500–800 PJ globally [3]. A large portion of this energy demand is met by fossil fuels, with thermal energy accounting for 85% of total demand in the EU [1] and 75% in the US [4]. From an environmental perspective, the glass industry is responsible for over 85 million tons of CO2 emissions globally [5], including 22 million tons in Europe [6], and 15 million tons in the US [4]. The primary sources of emissions include process emissions from the oxidation of carbon from raw materials, direct emissions from fuel combustion, and indirect emissions from electricity consumption. Direct and indirect energy-related emissions together account for more than 75% of total emissions across major glass products [7], thus making energy a hotspot for the decarbonisation of the sector.

Driven primarily by increased energy costs, the energy performance of glassmaking has improved significantly over the last century, approaching the physical limits of the performance of conventional furnaces [8]. The increased environmental awareness has focused attention on the carbon footprint of energy use, requiring a shift from fossil fuels to renewable energy sources. However, the low energy density and intermittent nature of the latter make adaptation to the continuous and energy-intensive process activities of the glass industry very challenging.

To this purpose, some studies have discussed the potential of biofuels [9], whereas others have focused on the combination of renewable electricity and green hydrogen [10]. The latter solution can leverage the dual energy input of hybrid furnaces to significantly reduce energy-related emissions. While a carbon-free electrical input is limited by the intermittency of renewable energy availability, hydrogen offers a solution for a decarbonised fuel input by decoupling energy supply and demand, albeit at the cost of overall energy efficiency [7].

Hybrid glass furnaces can be designed to operate over a wide range of electrical input, up to 80%. Furnaces are typically operated at constant boosting levels due to the relevant implications for heat flux distribution, convection currents, and melting processes that occur particularly at low combustion inputs [11]. Investigating the optimal ratio between fuel and electric inputs becomes very important, particularly for purposes of renewable energy integration.

This work analyses the impact of increased electric boosting and solar energy availability in hybrid glass furnaces, using a representative 300 t/d oxyfuel furnace as a case study. Economic and environmental thresholds for electrification are identified and compared with current energy prices and carbon emission factors. Then, a mixed-integer linear programming (MILP) formulation is employed to investigate optimal solar and hydrogen integration in terms of economic, environmental and renewable energy integration performance. The primary aim is to identify sizing guidelines that can support industrial actors in the design of low-carbon glass melting furnaces while minimising burdens on the broader energy system.

2 Energy Demand of Glass Furnaces

2.1 Glass Furnaces and Decarbonisation Pathways

Melting, fining, refining, and conditioning are essential steps carried out in glass furnaces. These processes involve heating the batch to its melting point, promoting fusion reactions to generate the melt, dissolving sand grains, eliminating bubbles, and achieving chemical and thermal homogenisation. The melting temperature is approximately 1500 ℃, with most of the enthalpy required in the primary batch-to-melt conversion. The chemical enthalpy required accounts for only 10–15% at typical industrial levels of glass cullet.

Several types of glass furnaces are available for various types of glass products, including recuperative, regenerative cross-fired and end-port, oxyfuel, and all-electric furnaces [12]. These vary in terms of how energy is supplied to glass, the amount of energy recovery, but also in the different convection cells and the consequent hot spot. The resulting specific energy consumption (SEC) varies significantly depending on product type, but also on production scale [7].

Several solutions have been developed to increase the energy efficiency of glass melting. Selective batching and the use of glass cullet can reduce the chemical enthalpy of the glass batch. To recover thermal energy from flue gas several solutions have been implemented, including batch and cullet preheating, thermochemical recuperation, steam generation, or electricity generation through organic Rankine cycles. More structural solutions aimed at reducing flue gas losses include oxyfuel combustion and all-electric melting, which reduce flue gas volumes partially and entirely, respectively.

Beyond energy efficiency solutions, biogas and renewable electricity represent viable alternatives for clean energy supply in glass furnaces. Renewable electricity can be supplied directly to furnace electrodes or used to produce green hydrogen for combustion in burners.

2.2 Case Study and System Layout

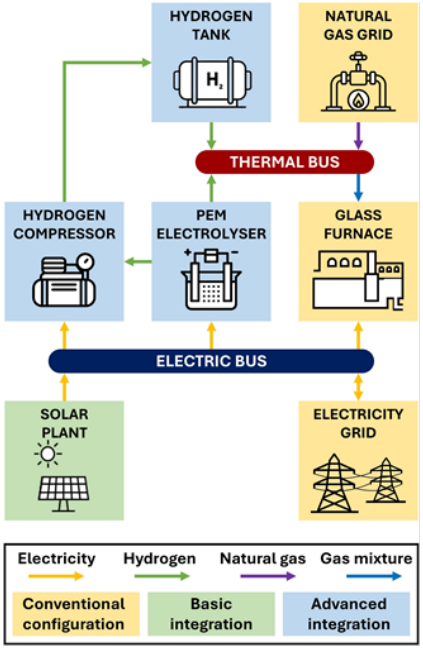

Figure 1. System layout

This work uses a 300 t/d oxyfuel container glass furnace with a nominal boosting power of 1 MW as a case study. The SEC is equal to 4.35 GJ/t, consisting of 3.8 GJ/t of fuel input, 0.29 GJ/t of electric input, and 0.26 GJ/t required for oxygen generation [13]. The thermodynamic efficiency is about 50%, energy losses due to flue gases and wall losses are 27% and 23%, respectively.

The overall system layout is shown in Figure 1 for three different configurations. The yellow elements represent the conventional configuration of a hybrid glass furnace, where burners and boosting electrodes are fed from the natural gas and electricity grids, respectively. A basic integration configuration considers the direct coupling of the furnace with photovoltaic modules. The advanced integration scenario consists of a hydrogen infrastructure including a PEM electrolyser to produce hydrogen and a pressurised hydrogen tank equipped with a hydrogen compressor. In the advanced integration scenario, electricity generated by the solar plant can be directed to the furnace electrodes, used by the electrolyser to partially offset excess renewable output, or fed into the electricity grid.

3 Energy Modelling

An MILP optimisation framework is proposed to optimise the operation of the system considered. This Section outlines the main components modelling choices, the MILP formulation, and the definition of the key performance indicators (KPI) for comparing the results across different configurations.

3.1 Components Modelling

3.1.1 Glass furnace

SEC variations of the furnace at different boosting ratios are assumed to vary linearly between the nominal condition and the 100% boosting condition, the latter corresponding to an SEC of 2.8 GJ/t due to the elimination of energy losses through flue gases. The resulting SEC under varying boosting ratio is reported in Table 1. The obtained results are conservative with respect to a 320 t/d oxyfuel furnace that is estimated to reach 2.6 GJ/t for a boosting ratio of around 67% [14].

Table 1. SEC under varying boosting ratio

Electric Boosting [%]	SEC [GJ/t]	Fuel Input [GJ/t]	Electric Input [GJ/t]
7	4.09	3.80	0.29
10	4.05	3.65	0.41
20	3.93	3.15	0.79
30	3.82	2.67	1.14
40	3.70	2.22	1.48
50	3.58	1.79	1.79
60	3.46	1.38	2.08
70	3.34	1.00	2.34
80	3.22	0.64	2.58

3.1.2 Renewable plant

The study considers different sizes of the solar plant. The energy coverage is assumed to range from 25% to 150% of the furnace's nominal annual energy demand in its conventional configuration (including oxygen energy requirements), which is around 124 GWh/y. This approach enables the evaluation of various renewable energy integration scenarios in the glass industry. The nominal power of the solar plant W_s can be expressed as in Eq. (1). where SEC_{nom} is the nominal SEC expressed in MWh/t, tpd_{nom} is the nominal production capacity of 300 t/d, EC is the energy coverage (ranging between 0.25 and 1.5), and CF is the photovoltaic modules' capacity factor, expressed in equivalent hours.

$$W_S = \left(SEC_{nom} \cdot tpd_{nom} \cdot EC \cdot 365\right) / CF \tag{1}$$

A single solar plant installed at or near the furnace site can hardly cover a significant portion of the energy demand of a glass furnace, due to its energy-intensive nature. Accordingly, rather than using the output profile of a single plant representative of a specific location, this study considers national-level nominal generation profiles [15]. The furnace is assumed to be located in Italy, so the capacity factor for solar is equal to 1122 hours [16]. For a 1:1 ratio between energy generation and energy demand, the associated rated power of the solar plant corresponds to a value of 110.82 MW. It is important to note that even for a boosting ratio of 80% the furnace electrical nominal power reaches only 8.84 MW, implying that a large oversizing of the solar plant is required.

Considering the mismatch between furnace energy demand and solar energy generation under varying plant size, excess energy on a daily scale is observed only when renewable energy coverage is at least 75%. However, it should be noted that, on an hourly scale, a small energy surplus occurs during the hottest period even at an energy coverage level as low as 25%.

3.1.3 Hydrogen infrastructure

The advanced integration configuration includes a PEM electrolyser and a hydrogen compressor and storage tank.

The sizing of the PEM electrolyser depends on a trade-off between overall operational efficiency and total hydrogen production. To derive general guidelines, it can be parametrised depending on renewable energy availability [17]. In most studies, hydrogen allocation is fixed to a certain threshold in order to promote economic viability [18]. However, to ensure a fair comparison between electrification and hydrogen for the glass industry, it is essential that no arbitrary prioritisation is performed.

The electrolyser is modelled to operate in the range of 15–100% of nominal input power, with an efficiency expressed as Eq. (2), adapted from the relation proposed in reference [19].

$$\eta_{PEM} = -0.149 \cdot W_{PEM}/W_{PEM,nom} + 74.977 \tag{2}$$

where, η_{PEM} is the electrolyser efficiency, W_{PEM} is the electrolyser input power, $W_{PEM,nom}$ is the nominal input power.

A hot standby battery is assumed to be installed to maintain the electrolyser ready to resume operation without delays. It is estimated that during non-productive hours the power consumption is equal to 1.5% of the electrolyser nominal power [18]. For the sizing of the hydrogen tank, a storage capacity of 3 days is considered to match with the optimisation horizon described in the following section. For the hydrogen compressor up to 200 bar, a specific energy consumption of 4 MJ/kg is assumed [20]. Following a stoichiometric reaction, it is assumed that 9 kg of water are required to produce 1 kg of hydrogen, with a lower heating value (LHV) of 120 MJ/kg.

3.2 Mixed Integer Linear Programming Formulation

An optimisation problem is formulated to determine the optimal hourly energy supply of the hybrid glass furnace, with the objective of minimising melting costs. An MILP approach is chosen as it is well suited to the problem's linear objective function and constraints, ensuring the identification of the global optimum. The optimisation is solved with an hourly time resolution considering a 7-days horizon in order to account for the variability of renewable energy generation. The optimisation problem is defined as in Eq. (3).

$$\min \left(\Sigma^T f_{obj}(x)\right)_{x \in Q \in R} \tag{3}$$

where, f_{obj} is the objective function, T is the weekly optimisation horizon, x is the vector of N optimisation variables, and Ω the feasible space delimited by the set of constraints.

Glass melting costs are chosen as the objective function , as shown in Eq. (4), including costs of natural gas and electricity purchases obtained by multiplying the purchase volumes Q_{in} and W_{in} by their specific prices c_{ng} and c_{el}, the revenues from electricity sales obtained by multiplying the sales volumes W_{out} by the electricity sales price $c_{el,out}$, the costs of direct carbon emissions obtained by multiplying the natural gas input by the CO_2 emission factor $CO_{2,f}$ and the price of CO_2 c_{CO_2}, and the cost of oxygen and water obtained by multiplying their purchase volumes $O_{2,in}$ and H_2O_{in} by their prices CO_2 and c_{H2O}.

$$f_{obj} = \Sigma_t^T \left(Q_{in} \cdot c_{ng} + W_{in} \cdot c_{el} - W_{out} \cdot c_{el,out} + Q_{in} \cdot \mathrm{CO}_{2,f} \cdot c_{\mathrm{CO2}} + O_{2,in} \cdot c_{\mathrm{O2}} + \mathrm{H_2O}_{in} \cdot c_{\mathrm{H2O}}\right) \tag{4}$$

The optimisation problem is constrained by a set of constraints. The constraint on the electric bus is expressed as in Eq. (5), where W_S is the hourly solar power generation, W_{PEM} is the power consumption of the electrolyser, $W_{PEM,standby}$ is the power consumption of the electrolyser due to the hot-standby during non-working hours, W_{H2C} is the power consumption of the hydrogen compressor, W_{in} and W_{out} are the purchase and sales to the electricity grid, and W_{fur} represents the furnace electrical input.

$$W_S - W_{PEM} - W_{PEM,standby} - W_{H2C} + W_{in} - W_{out} - W_{fur} = 0 \tag{5}$$

The constraint on the thermal bus is expressed as in Eq. (6), where Q_{PEM} is the energy content of PEM hydrogen generation, $Q_{H2S,ch}$ and $Q_{H2S,dis}$ represent the charge and discharge of the hydrogen tank, Q_{in} is the purchase from the natural gas grid, and Q_{fur} represents the furnace thermal input.

$$Q_{PEM} - Q_{H2S,ch} + Q_{H2S,dis} + Q_{in} - Q_{fur} = 0 \tag{6}$$

The operation of the hydrogen storage is modelled as suggested in reference [21] by imposing some constraints built with integer optimisation variables that control the on–off status of the storage, and the mutually exclusive charging or discharging mode. The state of charge of the storage tank is constrained to be equal at the beginning and the end of the optimisation horizon.

3.3 Key Performance Indicators

The three configurations are compared in terms of the economic and environmental performance as well as the self-sufficiency of renewable energy integration.

Specific melting costs defined as a yearly average of natural gas and electricity purchase C_{ng} and C_{ng}, electricity sale S_{el}, CO_2 quotas from the carbon market C_{CO2}, and oxygen and water purchase CO_2 and C_{H2O} are used as the economic KPI, KPI_{eco}, as shown in Eq. (7). The electricity and natural gas prices are selected from the first semester of 2024 for the corresponding consumption band of non-household consumers and are equal to 167.7 EUR/MWh and 51.4 EUR/MWh, respectively [22, 23]. The selling price of electricity is assumed to be 10% of the purchase price to encourage self-consumption and minimise grid interaction. The cost of oxygen is assumed to be 0.05 EUR/kg [20], the cost of water is assumed to be and 3.58 EUR/m^3 [18]. The cost of CO_2 is assumed to be 75 EUR/t, in line with 2025 forecasts.

Specific emissions, defined as a yearly average of natural gas emissions E_{ng} and electricity indirect emissions E_{el}, are used as the environmental KPI, KPI_{env}, as shown in Eq. (8).

For renewable energy integration, two indicators are considered, namely the self-consumption and self-production rates, KPI_{sc} and KPI_{sp}. Self-consumption rates measure the share of energy used within the designed system and are defined as the ratio of annual solar energy generation W_S minus the electricity sale $W_{el,out}$ over the sum of solar energy generation W_S, as shown in Eq. (9). Self-production rates measure the share of energy produced by the solar plant in the total energy supply and are defined as the ratio of annual solar energy generation W_S minus the electricity sale $W_{el,out}$ over the sum of solar energy generation W_S, natural gas purchase Q_{in} and electricity purchase W_{in}, as shown in Eq. (10). By definition, self-consumption rates will be larger than self-production rates since the denominator of the latter includes grid energy inputs.

$$KPI_{eco} = \left[\Sigma_t^T \left(C_{ng} + C_{el} - S_{el} + C_{CO2} + C_{O2} + C_{H2O}\right)\right] / \left(tpd_{nom} \cdot T\right) \tag{7}$$

$$KPI_{env} = \left[\Sigma_t^T \left(E_{ng} + E_{el}\right)\right] / \left(tpd_{nom} \cdot T\right) \tag{8}$$

$$KPI_{sc} = \left[\Sigma_t^T \left(W_S - W_{out}\right)\right] / \Sigma_t^T W_S \tag{9}$$

$$KPI_{sp} = \left[\Sigma_t^T \left(W_S - W_{out}\right)\right] / \left[\Sigma_t^T \left(W_S + Q_{in} + W_{in}\right)\right] \tag{10}$$

4 Results

This Section presents the results in terms of the economic, environmental and renewable-related KPIs for the three configurations of conventional natural gas fired furnace, direct coupling integration with solar photovoltaic, and advanced integration through a hydrogen infrastructure.

4.1 Conventional Configuration

The production of glass is very sensitive to the price of energy, as energy costs account for between 20% and 35% of total production costs depending on glass sub-sectors [24]. In this regard, Table 2 shows glass melting costs based on the natural gas and electricity prices in the first semester of 2018 and 2024 for the four main EU glass producing countries, i.e., Germany, Spain, France, and Italy. These data reflect glass melting prices without carbon pricing and show the relevant increase between the two periods considered, ranging from 30% in Spain to more than 75% in Germany.

Table 2. Melting costs in the conventional configuration in the main EU glass producing countries

[EUR/t]	Germany	Spain	France	Italy
2018-S1	57.25	55.67	55.03	51.13
2024-S1	110.7	72.31	81.05	82.98
Ratio (2024/2018)	1.76	1.30	1.47	1.62

Energy prices not only influence the cost of melting, but also the viability of decarbonisation options such as electrification. Indeed, electrification only provides environmental benefits if electricity is generated from clean energy sources. Based on the SEC of Table 1, the electricity price and emission factor thresholds below which electrification is economically and environmentally advantageous compared to natural gas can be expressed as Eq. (11) and Eq. (12). Here, a_1 results from the electrification benefits in terms of energy efficiency and is equal to 1.51. This value represents the maximum price ratio between electricity and natural gas for which electrification is convenient in the absence of any carbon tax. Assuming a carbon emissions factor of 0.2 tCO_2//MWh for natural gas combustion, electricity results in a net emission reduction only when its emission factor is below 0.30 tCO_2/MWh if emissions for oxygen generation are included.

$$c_{el,thr} = a_1 \cdot (c_{ng} + \mathrm{CO}_{2,f} \cdot c_{\mathrm{CO2}}) \tag{11}$$

$$em_{el,thr} = a_1 \cdot em_{ng} \tag{12}$$

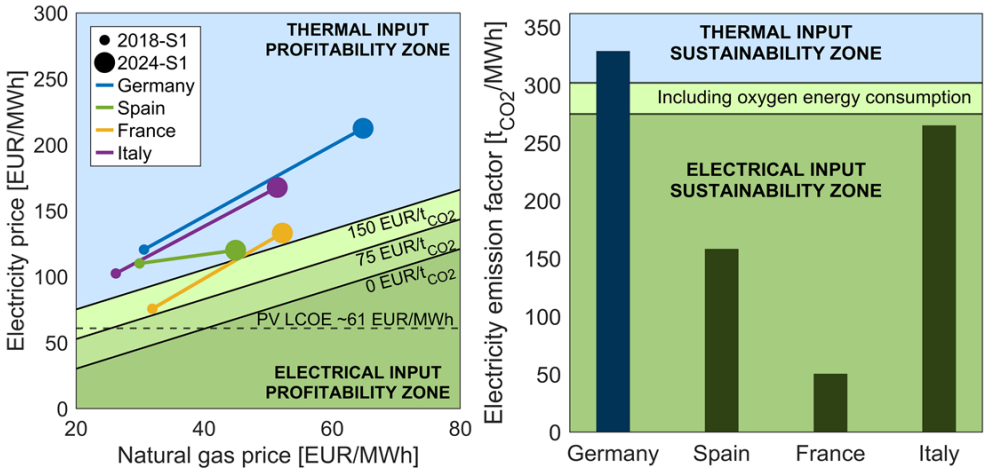

(a) Economic viability (b) Environmental viability

Figure 2. Profitability and sustainability zones of energy inputs compared with current energy prices and electricity carbon emission factors in the main EU glass producing countries

Figure 2 shows the profitability and sustainability zones of the electrical and thermal inputs compared to the energy prices and emission factors in the main EU glass producing countries. At current energy prices, natural gas maintains its economic advantages for all the countries considered, even for a carbon tax of 150 EUR/t. The price increase has been proportionally more relevant for electricity for most countries, thus acting as a disincentive to electrification. From an environmental perspective, electrification using national grids is sustainable for all the relevant glass producing countries except for Germany.

With purposes of renewable energy integration, current electricity prices can be compared to the levelised cost of electricity (LCOE) for solar energy generation, whose average in the countries considered is equal to around 60 EUR/MWh. This suggests that the availability of solar electricity for glass melting represents an important incentive for the electrification of the glass industry. If no carbon tax is considered, solar-powered electrification becomes convenient for natural gas prices above around 40 EUR/MWh, which is the case for all the main EU glass producers. This threshold further decreases in case of a relative importance of the carbon tax, reaching around 25 EUR/MWh for a carbon tax of 75 EUR/t.

Concerning the furnace chosen as a case study, Table 3 reports the specific melting costs and carbon emissions including oxygen production costs and associated emissions. For boosting levels of 80%, melting costs increase by

around 35% with respect to the nominal configuration. On the contrary, carbon emissions are only slightly reduced since the average electricity emission factor of Italy is assumed to be equal to 0.265 tCO_2/MWh based on the carbon footprint and the amount of energy generated by different technologies in Italy [25].

Table 3. Melting costs and carbon emissions under varying furnace electric boosting in Italy

Electric Boosting [%]	Melting Costs [EUR/t]	Carbon Emissions [kg_{CO_2}/t]
7	98.65	0.249
10	100.7	0.249
20	107.25	0.248
30	113.23	0.246
40	118.63	0.243
50	123.46	0.240
60	127.72	0.237
70	131.41	0.233
80	134.52	0.229

4.2 Solar Integration

The direct integration configuration consists of coupling the hybrid glass furnace with the solar plant while the advanced integration configuration consists of a PEM electrolyser, a hydrogen storage tank, and a hydrogen compressor. In the latter configuration, surplus energy produced by the solar plant can be employed to produce hydrogen, thereby covering a part of thermal energy demand.

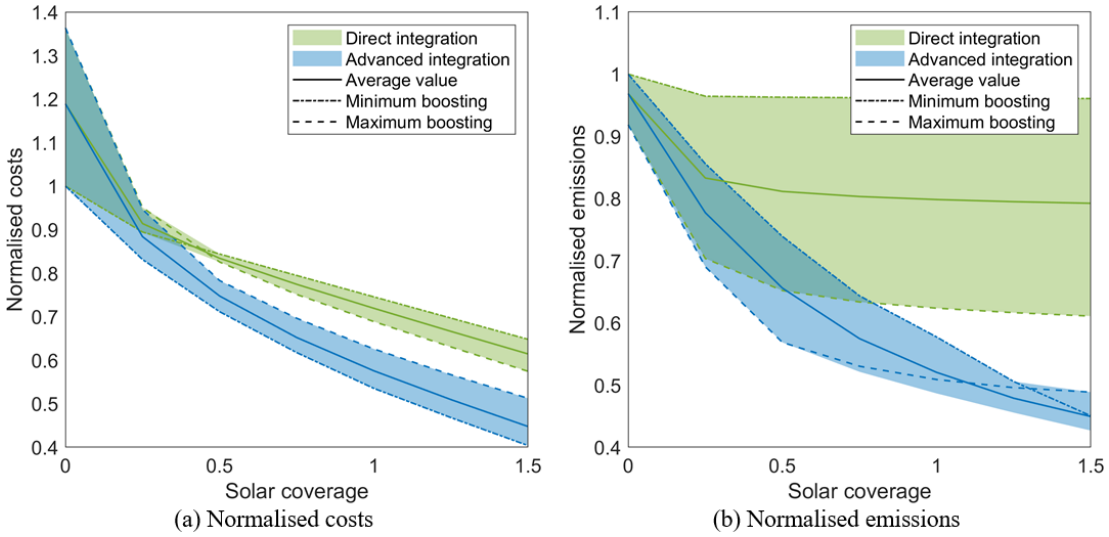

(a) Normalised costs (b) Normalised emissions

Figure 3. Basic and advanced integration economic and environmental KPIs under varying solar coverage

Figure 3 shows the comparison of the economic and environmental performance of the basic and advanced integration configurations under varying solar coverage, normalised with respect to the nominal configuration of 7% boosting and absence of solar energy coverage. As can be seen, both costs and emissions can be significantly reduced for increasing levels of solar coverage.

From an economic perspective, the profitability of increased boosting levels in the basic integration configuration is achieved only for solar coverage levels higher than 50%. On the contrary, in the advanced integration configuration optimal reductions are achieved for minimum boosting levels across all solar energy coverage levels. At a solar coverage of 1:1 with the nominal furnace energy demands, the basic integration yields melting costs reductions ranging from 25.5% at low boosting levels to 31.1% at high boosting levels. In the advanced integration configuration, cost reductions range from 46.5% for a boosting ratio of 7% to 37.4% for a boosting ratio of 80%.

From an environmental perspective, in the direct integration configuration electrification yields emission reductions across all solar energy coverage levels. In the advanced configuration, higher solar energy availability shifts the maximum reductions towards lower electrification levels. At an energy demand-supply ratio of 1:1, the basic configuration yields maximum emission reduction of 37.6% whereas the advanced integration yields maximum reductions of 49.1%.

From the perspective of renewable energy integration, Figure 4 shows the self-consumption and self-production rates in the direct and advanced integration configurations under varying solar coverage. In the basic integration configuration, maximum self-consumption and self-production rates are achieved for the maximum boosting ratio and a solar energy coverage of 25%, reaching values of 84.0% and 25.3%, respectively. The implementation of a hydrogen infrastructure allows a significant increase in both KPIs, also causing a shift in the optimal solution from high to low levels of boosting. At a solar coverage level of 100%, self-consumption shares are increased from the values of 3.5% and 27.7% at minimum and maximum boosting levels, to values of 95.9% and 56.0%, respectively. At a solar coverage level of 100%, self-production shares are increased from the values of 1.8% and 18.4% at minimum and maximum boosting levels, to values of 62.8% and 40.4%, respectively.

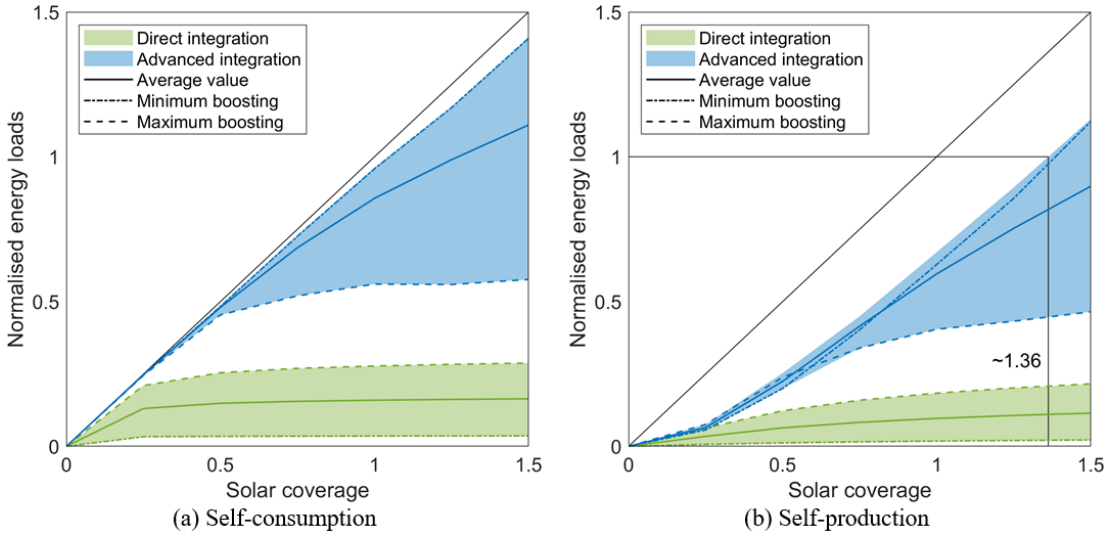

Figure 4. Basic and advanced integration self-consumption and self-production rates under varying solar coverage

For the glass furnace under analysis, it can also be estimated that around 36% of solar overgeneration is required for the glass furnace to be completely self-sufficient. This corresponds to a capacity of the solar park equal to 150 MW and an electrolyser capacity of around 45 MW. For boosting levels between 7% and 20%, overgeneration requirements span the range of 36–40%, highlighting a moderate impact of the boosting level for self-sufficiency in low electrification scenarios.

5 Conclusions

This study has explored the decarbonisation of the glass industry through direct and hydrogen-based electrification based on different levels of solar energy availability.

Economic and environmental thresholds for the viability of increased electric boosting in glass furnaces were investigated, considering the differing energy efficiency of thermal energy supplied by fuel burners versus electrodes within hybrid furnaces. Specifically, electrification becomes advantageous when the electricity-to-natural-gas price ratio is below 1.5 and the electricity emission factor is under 0.3 tCO_2/MWh. However, current energy price conditions in major EU glass-producing countries show that increased electric boosting is currently not economically viable, even under carbon taxes as high as 150 EUR/t. In contrast, the carbon intensity of national electricity mixes in these countries would allow for net emissions reductions.

Optimal solar integration has been investigated in terms of economic, environmental, and renewable integration KPI with regard to a representative 300 t/d hybrid oxyfuel glass furnace located in Italy, comparing three different configurations: a conventional natural gas-fired hybrid furnace, a direct electrification scenario using solar photovoltaics, and an advanced integration configuration incorporating green hydrogen via a proton exchange membrane electrolyser. A techno-economic evaluation based on mixed integer linear programming was conducted across boosting levels ranging from 7% to 80% and solar plant sizing of up to 150% of the furnace's nominal energy demand. The results are evaluated in terms of KPI, including melting costs, specific emissions, and self-consumption and self-production rates.

Under direct solar integration, at a supply-to-demand ratio of 1:1, melting cost savings peaked at 31.1%, while carbon emissions were reduced by up to 37.6%. Daily mismatches between intermittent solar generation and the furnace continuous energy demands limited self-consumption rates and self-production rates to 27.7% and 18.4%. In the advanced integration configuration, hydrogen offers a solution to decouple energy supply and demand, maximising the self-sufficiency of the energy system considered. Melting cost savings reach 46.8% at minimum

boosting levels, while carbon emission reductions exhibit maximum values of 51.3% at 60% boosting. The hydrogen infrastructure enables increased self-consumption and self-production rates up to 96.3% and 67.0% at boosting levels of 10% and 40%, respectively.

Furthermore, for low boosting levels (between 7% and 20%), the required solar overgeneration amounts to around 36–40%, offering a practical guideline for targeting optimal integration of solar energy in the glass industry. For the 300 t/d oxyfuel furnace considered as a case study, a solar plant with a capacity of around 150 MW and an electrolyser capacity of around 45 MW are necessary for achieving full energy self-sufficiency.

This evaluation provides a detailed, bottom-up modelling framework to assess energy transition pathways in the glass industry. A clear trade-off emerges between electrification and hydrogen strategies, as the latter achieves better results at minimum values of furnace electric input. Since results are highly context-dependent, future work should conduct sensitivity analyses on energy prices, and carbon permit costs and include the analysis of capital expenditures for technologies involved.

Funding

This work was supported by the National Recovery and Resilience Plan (NRRP), Mission 4 Component 2 Investment 1.3—Call for tender No. 1561 of 11.10.2022 of Ministero dell'Università e della Ricerca (MUR); project funded by the European Union—NextGenerationEU. Award Number: Project code PE0000021, Concession Decree No. 1561 of 11.10.2022 adopted by Ministero dell'Università e della Ricerca (MUR), CUP I53C22001450006, according to attachment E of Decree No. 1561/2022, Project title "Network 4 Energy Sustainable Transition—NEST".

Data Availability

The data used to support the findings of this study are available from the corresponding author upon request.

Conflicts of Interest

The authors declare that they have no conflicts of interest.

References

[1] A. Schmitz, J. Kamiński, B. M. Scalet, and A. Soria, "Energy consumption and CO_2 emissions of the European glass industry," *Energy Policy*, vol. 39, no. 1, pp. 142–155, 2011. https://doi.org/10.1016/j.enpol.2010.09.022

[2] U.S. Department of Energy, "Bandwidth study U.S. glass manufacturing," 2017. https://www.energy.gov/eere/iedo/articles/bandwidth-study-us-glass-manufacturing

[3] International Energy Agency, "Tracking industrial energy efficiency and CO_2 emissions," 2007. https://www.iea.org/reports/tracking-industrial-energy-efficiency-and-co2-emissions

[4] U.S. Department of Energy, "Manufacturing energy and carbon footprints," 2018. https://www.energy.gov/eere/iedo/manufacturing-energy-and-carbon-footprints-2018-mecs

[5] J. Eid, "Glass is the hidden gem in a carbon-neutral future," *Nature*, vol. 599, pp. 7–8, 2021. https://doi.org/10.1038/d41586-021-02992-8

[6] European Climate, Infrastructure and Environment Executive Agency, "How LIFE is reducing emissions from glass production," 2022. https://cinea.ec.europa.eu/news-events/news/how-life-reducing-emissions-glass-production-2022-03-16_en

[7] L. Miserocchi, A. Franco, and D. Testi, "Status and prospects of energy efficiency in the glass industry: Measuring, assessing and improving energy performance," *Energy Convers. Manag. X*, vol. 24, p. 100720, 2024. https://doi.org/10.1016/j.ecmx.2024.100720

[8] R. Conradt, "Prospects and physical limits of processes and technologies in glass melting," *J. Asian Ceram. Soc.*, vol. 7, no. 4, pp. 377–396, 2019. https://doi.org/10.1080/21870764.2019.1656360

[9] P. W. Griffin, G. P. Hammond, and R. C. McKenna, "Industrial energy use and decarbonisation in the glass sector: A UK perspective," *Adv. Appl. Energy*, vol. 3, p. 100037, 2021. https://doi.org/10.1016/j.adapen.2021.100037

[10] M. Zier, N. Pflugradt, P. Stenzel, L. Kotzur, and D. Stolten, "Industrial decarbonization pathways: The example of the German glass industry," *Energy Convers. Manag. X*, vol. 17, p. 100336, 2023. https://doi.org/10.1016/j.ecmx.2022.100336

[11] W. Kuhn, A. Reynolds, P. Molcan, and B. Malphettes, "Electric boosting and hybrid furnaces (practical application of higher levels of electric heat input)," in *80th Conference on Glass Problems*. Wiley, 2021, pp. 53–69. https://doi.org/10.1002/9781119744931.ch6

[12] C. Jatzwauk, "Design and operation of glass furnaces," in *Encyclopedia of Glass Science, Technology, History, and Culture*. Wiley, 2021, pp. 1147–1164. https://doi.org/10.1002/9781118801017.ch9.7

[13] H. Kobayashi, "Future of oxy-fuel glass melting: Oxygen production, energy efficiency, emissions and CO_2 neutral glass melting," in *80th Conference on Glass Problems*. Wiley, 2021, pp. 1–12. https://doi.org/10.1002/9781119744931.ch1

[14] H. P. H. Muijsenberg, H. Mahrenholtz, P. Jandacek, S. Hakes, and C. Jatzwauk, "Carbon reduction with super boosting and advanced energy management using renewable resources," in *80th Conference on Glass Problems*. Wiley, 2021, pp. 71–93. https://doi.org/10.1002/9781119744931.ch7

[15] ENTSO-E, "Transparency Platform," 2025. https://newtransparency.entsoe.eu/

[16] TERNA, "Dati Statistici," 2025. https://dati.terna.it/generazione/dati-statistici/

[17] P. Marocco, M. Gandiglio, R. Cianella, M. Capra, and M. Santarelli, "Design of hydrogen production systems powered by solar and wind energy: An insight into the optimal size ratios," *Energy Convers. Manag.*, vol. 314, p. 118646, 2024. https://doi.org/10.1016/j.enconman.2024.118646

[18] A. Franco, C. Carcasci, A. Ademollo, M. Calabrese, and C. Giovannini, "Integrated plant design for green hydrogen production and power generation in photovoltaic systems: Balancing electrolyzer sizing and storage," *Hydrogen*, vol. 6, no. 1, p. 7, 2025. https://doi.org/10.3390/hydrogen6010007

[19] A. Hofrichter, D. Rank, M. Heberl, and M. Sterner, "Determination of the optimal power ratio between electrolysis and renewable energy to investigate the effects on the hydrogen production costs," *Int. J. Hydrogen Energy*, vol. 48, no. 5, pp. 1651–1663, 2023. https://doi.org/10.1016/j.ijhydene.2022.09.263

[20] P. Marocco, M. Gandiglio, D. Audisio, and M. Santarelli, "Assessment of the role of hydrogen to produce high-temperature heat in the steel industry," *J. Clean. Prod.*, vol. 388, p. 135969, 2023. https://doi.org/10.1016/j.jclepro.2023.135969

[21] A. Ghilardi, G. F. Frate, K. Kyprianidis, M. Tucci, and L. Ferrari, "Brayton pumped thermal energy storage: Optimal dispatchment in multi-energy districts," *Energy Convers. Manag.*, vol. 314, p. 118650, 2024. https://doi.org/10.1016/j.enconman.2024.118650

[22] Eurostat, "Electricity prices for non-household consumers - bi-annual data," 2025. https://doi.org/10.2908/NRG_PC_205

[23] Eurostat, "Gas prices for non-household consumers - bi-annual data," 2025. https://doi.org/10.2908/NRG_PC_203

[24] Glass Alliance Europe, "Glass industry calls for urgent and robust EU support measures for the glass sector to face the on-going energy crisis," 2022. https://glassforeurope.com/wp-content/uploads/2022/11/Glass-Alliance-Europe-Position-paper-on-energy-crisis-20221115.pdf

[25] ISPRA, "Fattori di emissione per la produzione ed il consumo di energia elettrica in Italia," 2025. https://emissioni.sina.isprambiente.it/fattori-di-emissione-produzione-consumo-energia-elettrica/

Nomenclature

CFD	Computational fluid dynamics
CO_2	Carbon dioxide
H_2O	Water
KPI	Key performance indicator
LCOE	Levelised cost of electricity
LHV	Lower heating value
MILP	Mixed-integer linear programming
O_2	Oxygen
PEM	Proton exchange membrane
SEC	Specific energy consumption

Symbols

c	Specific cost, EUR·J
C	Cost, EUR
CF	Capacity factor
$\mathrm{CO}_{2,f}$	Carbon dioxide emission factor, t·J
EC	Energy coverage
f_{obj}	Objective function
Q	Thermal energy flow, J
R	Revenue, EUR
tpd	Pull rate, t·d
W	Electrical energy flow, J

Greek symbols

η	Efficiency

Subscripts

ch	Charge
dis	Discharge
eco	Economic
el	Electricity
env	Environmental
fur	Furnace
H_2C	Hydrogen compressor
H_2S	Hydrogen storage
in	Input
ng	Natural gas
nom	Nominal
out	Output
$standby$	Standby
S	Solar
sc	Self-consumption
sp	Self-production
t	Optimisation timestep
T	Optimisation horizon
thr	Threshold value